Supporting Information

Cortés et al. 10.1073/pnas.1118138109

SI Materials and Methods

Cells, cDNA, Antibodies, and Reagents. Murine embryonic fibroblasts (MEFs) and NIH 3T3, COS-7, HeLa, Jurkat, HT1080, BLM, and U2OS cells were cultured as reported previously (1). Lines stably expressing p85α or p85β were prepared as described previously (2). Cells were transfected with Lipofectamine (Invitrogen). p85β was subcloned into pSG5 and a hemagglutinin (HA) epitope was added in-frame at the N terminus. The p85β ATG codon was replaced with a CCG codon (proline) and the HA-tag ATG codon was maintained (Quik-Change mutagenesis kit; Stratagene). pSG5, pSG5-p85α, pSG5-myc-p110α, pSG5-myc-p110α, pEF-BOS-HA-p85α, pEF-BOS-HA-p85β, and retroviral PRV-IRES-GFP-p85β have been described previously (3–5). The pEGFP-PH-Btk plasmid was donated by T. Balla (National Institutes of Health, Bethesda, MD). The plasmid pT7/T3-U19 encoding murine p85β (6) was donated by J. W. G. Janssen (Institute fur Humangenetik, Heidelberg, Germany). To prepare pcDNA3-Δp85β, we deleted the BamHI site of pcDNA3, subcloned an EcoRI fragment including p85β sequence into the EcoRI site of pcDNA3, and deleted the region of interaction with p110 by using the restriction enzymes AflII and BamHI. siRNA for human p85β and control were from Invitrogen; siRNA for human p85α was from Dharmacon; shRNA for mouse p85β was from Origene. IL-6 and stem cell factor were from Peprotech; IL-3 was from eBioscience. Primary Ab for Western blots (WBs) were anti–phospho-(p)-protein kinase B (PKB; Ser473; Cell Signaling), anti–pan-p85 PI3K, anti-human p85α and anti-PKB (Upstate Biotechnology), anti-GST (Abcam), and anti-HA (12CA5; Babco); anti-CD4 and -CD8 were from Pharmingen, and anti–β-actin was from Sigma-Aldrich. p110α Ab was donated by A. Klippel (Atugen, Berlin, Germany).

To prepare anti-p85β antibodies, we immunized rats with a GST-fused N-terminal murine p85β fragment (residues 1–305). Rat hybridoma 1C8 was prepared as described previously (7). Antibodies were tested in ELISA, WB, and immunoprecipitation (IP) by using recombinant bacterial proteins or extracts of rp85β- or rp85α-expressing cells. Rat mAb 1C8 was affinity purified (Protein G Sepharose; GE Healthcare) and recognized endogenous levels of p85β, but not p85α, in WB and IP.

WB, IP, PI3K Assay, Focus Formation, Invasion Assay, and Confocal Microscopy. Human cell lines and tumors were lysed in RIPA buffer containing protease and phosphatase inhibitors; NIH 3T3 cells were lysed in RIPA or 1% Triton X (TX)-100 buffer (1). IP, PI3K assay, focus formation, and cell invasion have been described previously (1, 8). For immunofluorescence, cells were fixed in fresh 4% (wt/vol) paraformaldehyde in PBS solution (15 min), permeabilized in PBS solution with 1% BSA and 0.3% TX-100, and blocked with 1% BSA, 10% (vol/vol) goat serum, and 0.01% TX-100 in PBS solution (30 min). Cells were visualized using a 60× 1.3 numerical aperture (N.A.) oil objective on an Olympus Fluoview 1000 microscope.

Human Tumor Analysis. Breast carcinoma (BC) and colon adenocarcinoma (CC) and adjacent normal tissue samples were provided by the Tissue Bank Network funded by the Molecular Pathology Program of the Spanish National Cancer Center. CCs were classified according to modified Dukes criteria (D0 to DC). BCs were graded by using Bloom–Richardson criteria (grades 1–3), and classified as luminal A, B, HER2$^+$, or basal-type (9), according to expression of estrogen and estrogen receptors [determined by immunohistochemistry (IH)] and HER2 (determined by FISH). For classification of basal BC (9), we stained tumor sections by IH for cytokeratin 5/6 and for EGFR expression.

Mutational status of hotspot residues of *K-Ras* (G12, G13) and *PIK3CA* (E542, E545, H1047) was analyzed in BC and CC. Fresh tumor tissue samples were dissected manually, and genomic DNA was extracted by using the Puregene Blood Core Kit B (Qiagen). *K-Ras* exon 2 and *PIK3CA* exons 9 and 20 were amplified, and a SNaPShot reaction was performed by using the SNaPshot Multiplex Kit (Applied Biosystems) as described previously (10, 11). A fraction of the samples was also analyzed by Sanger sequencing of PCR products to confirm mutant sequences.

For WB, frozen tumor sections were extracted in RIPA lysis buffer (1); extracts (50 μg) from tumors and surrounding normal tissue were examined by WB using appropriate antibodies. WB signal intensity was normalized to that of actin [or to PKB for phosphorylated pPKB (pPKB)]. Mean normalized signals ± SD were obtained from three or four independent tests. Normalized p85 or pPKB signal in tumors was divided by that obtained in normal tissue; numbers <1 (decreased expression) were converted to inverse negative values.

For IH, we used anti-pPKB (Ser473) and -pS6 (Ser235/236) antibodies (Cell Signaling). For IH signal values, we measured signal intensity (pixels minus background) using ImageJ to convert the blue channel of the original RGB images to grayscale (specific peroxide signal). Signal intensity (scored as 1–3) was scored in tumor cells (score of 1, 0.5–1.5 × 10^5 pixels/cell; score of 2, 1.5–3 × 10^5 pixels/cell; score of 3, 3–6 × 10^5 pixels/cell). Signal intensity scores were multiplied by the percentage of pS6-positive tumor cells. When this value was <0.20 (samples with low signal intensity or with a low proportion of pS6-positive tumor cells), the sample was considered negative. For normalization with pPKB/PKB (i.e., tumor-to-normal) ratios, an IH signal of 0.20 was arbitrarily set at 1; all other IH values were scaled proportionally.

For quantitative PCR (qPCR), mRNA was obtained from frozen sections and examined in custom-designed TaqMan Low Density Arrays (Applied Biosystems) containing primers and probes for *GAPDH* (probe Hs4342376), *PIK3R1* (Hs00236128, Hs00381459), *PIK3R2* (Hs00178181), and *PTEN* (Hs00829813). As template for reverse transcription, 1 ng total RNA was used per sample (in triplicate). qPCR was performed on an ABI Prism 7900 HT system (Applied Biosystems). Relative mRNA quantification was done by calculating relative quantity (RQ) as $2^{-\Delta\Delta Ct}$, examining the cycle (i.e., Ct) at which the PCR product appears (normalized for *actin* and *GADPH* mRNA) for each gene. For miRNA analysis, TRIzol-extracted total RNA was retrotranscribed by using the TaqMan MicroRNA Reverse Transcription Kit (Applied Biosystems); *miR126* was measured by qPCR using specific probes (ID 002228; Applied Biosystems) and normalized to U6 snRNA (ID 001973; Applied Biosystems) and RNU19 controls (ID 001003; Applied Biosystems). For microarrays, biotinylated cDNA (10 μg) from the 12 CC and 14 BC samples and normal tissues was processed and hybridized to Human Genome Focus Arrays (Affymetrix). Arrays were scanned at 3-μm resolution in an HP G2500A GeneArray scanner (Agilent Technologies).

Mice, Bone Marrow Transfer, CC Model, and Lymphoma Model. p85β$^{-/-}$ mice were donated by D. Fruman (University of California, Irvine, CA), and BALB/c SCID mice were obtained from Jackson Laboratories; mice were bred and maintained in specific pathogen-free conditions in our animal facility. The Centro

Nacional de Biotecnología Ethics Committee approved all studies in accordance with national and European Union guidelines. For bone marrow (BM) transplants, BM was extracted from mouse femur, tibia, and humerus, and cells were disaggregated and washed. A BM suspension (10^7 cells/mL, 200 μL) was injected into the tail vein of irradiated (10 Gy) host mice (12). For spontaneous colorectal carcinogenesis in C57BL/6 WT and p85β$^{-/-}$ mice, animals were treated with azoxymethane/dextran sodium sulfate (13). As p85β$^{-/-}$ mice have a defective immune response (5), and carcinogenesis in this model depends on inflammation (13), mice were transplanted with WT BM as described earlier before azoxymethane treatment. At 3.5 mo after azoxymethane treatment, colons were resected and examined after H&E staining.

For comparison of thymic lymphomagenesis in SCID mice (14) expressing normal or high p85β levels, mice were transplanted with SCID or p85β-expressing SCID BM, maintained ∼1 mo for reconstitution, and then treated with N-ethyl-N-nitrosourea (ENU). Two-month-old WT BALB/c SCID donors were pretreated with 50 mg/kg 5-fluorouracil (4 d). BM was extracted and the cell suspension incubated (16 h) with DMEM plus 15% FCS, 5% WEHI cell line-conditioned medium (containing IL-3), 20 ng/mL recombinant IL-3, 100 ng/mL stem cell factor, and 10 ng/mL recombinant IL-6. Spin infection with control or p85β retroviruses (90 min, 37 °C) was performed by mixing cells with 2 mL retroviral supernatant with the cytokine mixture and 8 μg/mL Polybrene; infection was repeated after 16 h. At 72 h after the first infection, cells were injected (10^7 cells/mL, 200 μL) i.v. into irradiated BALB/c SCID mice (4.5 Gy). At 1 mo after transplantation, ENU was injected i.p. (0.5 μg/g in trioctanoin), which was repeated 2 wk later. Mice were maintained in an isolator; lymphoma development was first observed at 3 mo in p85β-transduced mice and at 7.5 mo in controls. Spleen and thymus were examined by flow cytometry and histochemistry.

BC Cell Line Analysis. BC cell lines MDA-MB231 and MDA-MB468 were cultured in DMEM or Leibovitz (L15) medium, respectively, containing 10% FBS. Cells were transfected with siRNA by using Lipofectamine RNAiMAX (Invitrogen). Cells were counted at different time points, and the number of viable cells was determined by trypan blue exclusion. Cell death was confirmed by measuring sub-G1 DNA containing cells by flow cytometry.

Statistical Analyses. Gel bands and IH and fluorescence intensity were quantified with ImageJ software. Associations between variables were assessed by correlation Pearson test, Fisher exact test, and χ^2 test. For multivariate Pearson test analysis, we used the IBM statistic 19 program. For mouse tumor analyses, we used Student *t* test and the Mantel–Cox test. For PI3K pathway evaluation, we used a Student *t* test. Except for multivariate analysis, all statistics were calculated by using Prism 5 version 5.0b software (GraphPad).

1. Marqués M, et al. (2008) Phosphoinositide 3-kinases p110alpha and p110beta regulate cell cycle entry, exhibiting distinct activation kinetics in G1 phase. *Mol Cell Biol* 28:2803–2814.
2. Jiménez C, et al. (2000) Role of the PI3K regulatory subunit in the control of actin organization and cell migration. *J Cell Biol* 151:249–262.
3. Jiménez C, Hernandez C, Pimentel B, Carrera AC (2002) The p85 regulatory subunit controls sequential activation of phosphoinositide 3-kinase by Tyr kinases and Ras. *J Biol Chem* 277:41556–41562.
4. Várnai P, et al. (2005) Selective cellular effects of overexpressed pleckstrin-homology domains that recognize PtdIns(3,4,5)P3 suggest their interaction with protein binding partners. *J Cell Sci* 118:4879–4888.
5. Alcázar I, et al. (2009) p85beta phosphoinositide 3-kinase regulates CD28 coreceptor function. *Blood* 113:3198–3208.
6. Janssen JW, Schleithoff L, Bartram CR, Schulz AS (1998) An oncogenic fusion product of the phosphatidylinositol 3-kinase p85beta subunit and HUMORF8, a putative deubiquitinating enzyme. *Oncogene* 16:1767–1772.
7. Kremer L, Márquez G (2004) Generation of monoclonal antibodies against chemokine receptors. *Methods Mol Biol* 239:243–260.
8. Molina-Ortiz I, Bartolomé RA, Hernández-Varas P, Colo GP, Teixidó J (2009) Overexpression of E-cadherin on melanoma cells inhibits chemokine-promoted invasion involving p190RhoGAP/p120ctn-dependent inactivation of RhoA. *J Biol Chem* 284:15147–15157.
9. Sørlie T, et al. (2001) Gene expression patterns of breast carcinomas distinguish tumor subclasses with clinical implications. *Proc Natl Acad Sci USA* 98:10869–10874.
10. Zinsky R, Bölükbas S, Bartsch H, Schirren J, Fisseler-Eckhoff A (2010) Analysis of KRAS mutations of exon 2 codons 12 and 13 by SNaPshot analysis in comparison to common DNA sequencing. *Gastroenterol Res Pract* 2010:789363.
11. Hurst CD, Zuiverloon TC, Hafner C, Zwarthoff EC, Knowles MA (2009) A SNaPshot assay for the rapid and simple detection of four common hotspot codon mutations in the PIK3CA gene. *BMC Res Notes* 2:66.
12. Balazs AB, Fabian AJ, Esmon CT, Mulligan RC (2006) Endothelial protein C receptor (CD201) explicitly identifies hematopoietic stem cells in murine bone marrow. *Blood* 107:2317–2321.
13. González-García A, Sánchez-Ruiz J, Flores JM, Carrera AC (2010) Phosphatidylinositol 3-kinase gamma inhibition ameliorates inflammation and tumor growth in a model of colitis-associated cancer. *Gastroenterology* 138:1374–1383.
14. Gurley KE, Vo K, Kemp CJ (1998) DNA double-strand breaks, p53, and apoptosis during lymphomagenesis in scid/scid mice. *Cancer Res* 58:3111–3115.

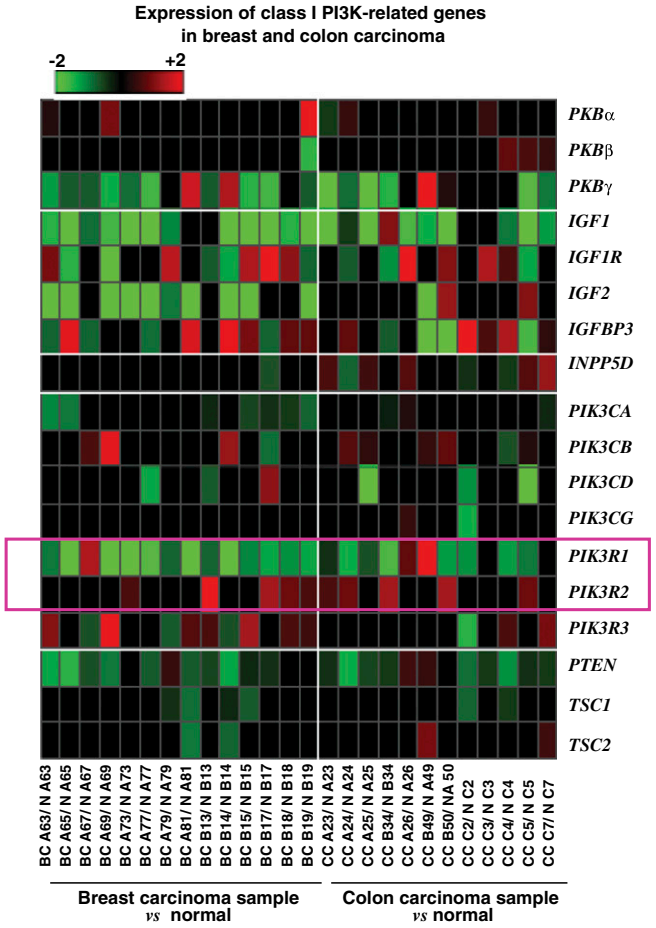

Fig. S1. PI3K pathway gene expression patterns in colon and breast carcinoma (CC and BC). Heat map representation of Affymetrix data, depicting PI3K pathway-related gene expression changes in BC or CC tumor samples vs. normal tissue. Microarray data are expressed as log-fold change in mRNA levels. Color code indicates increased (red) or decreased (green) levels in tumor.

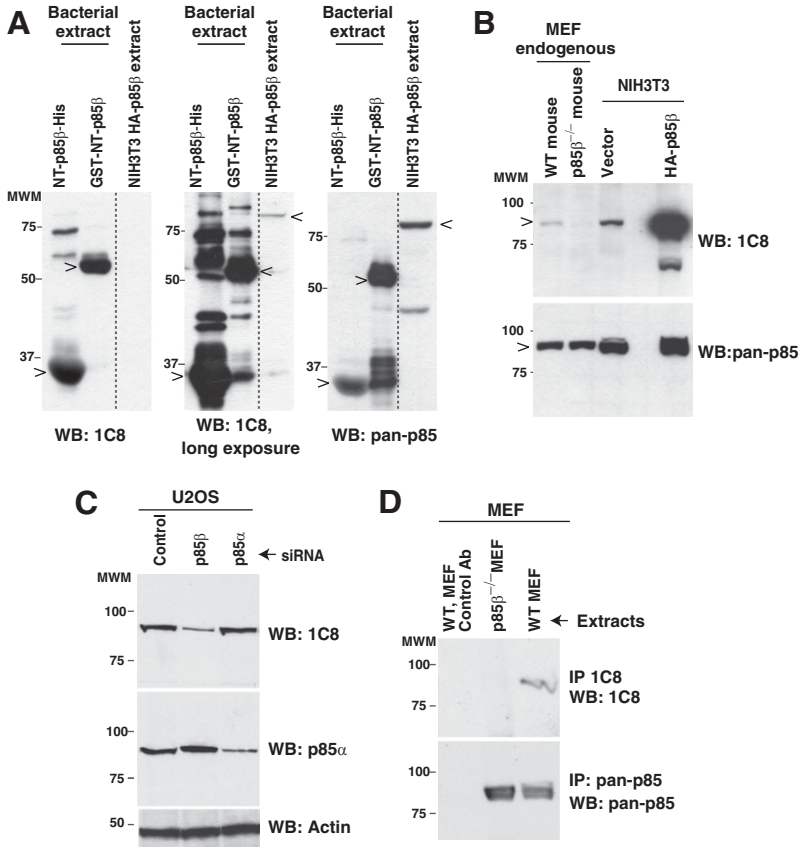

Fig. S2. Characterization of rat anti-p85β mAb 1C8. mAbs were selected in ELISA and positive clones characterized by IP and WB. (*A*) Extracts from bacteria expressing His-tagged murine N-terminal (NT) fragment of p85β, GST-NT-p85β, as well as extracts of NIH 3T3 cells expressing HA-p85β (indicated) were examined by WB with 1C8 Ab that recognized murine p85β, His-NT-p85β, and GST-NT-p85β. (*B*) Extracts from MEFs of WT or p85β$^{-/-}$ mice and extracts from control or p85β-expressing NIH 3T3 cells were examined as in *A*. mAb 1C8 selectively recognized endogenous murine p85β in MEF and NIH 3T3 cells (lanes 1 and 3). Arrowheads indicate specific bands. (*C*) Extracts of U2OS cells transfected with control, p85α-, or p85β-specific siRNA were examined as in *A*. (*D*) MEF extracts as in *B* were analyzed by IP with preimmune Ab (lane 1) or with 1C8 mAb or pan-p85 Ab as indicated. The 1C8 mAb was specific for the p85β isoform and recognized endogenous levels of p85β.

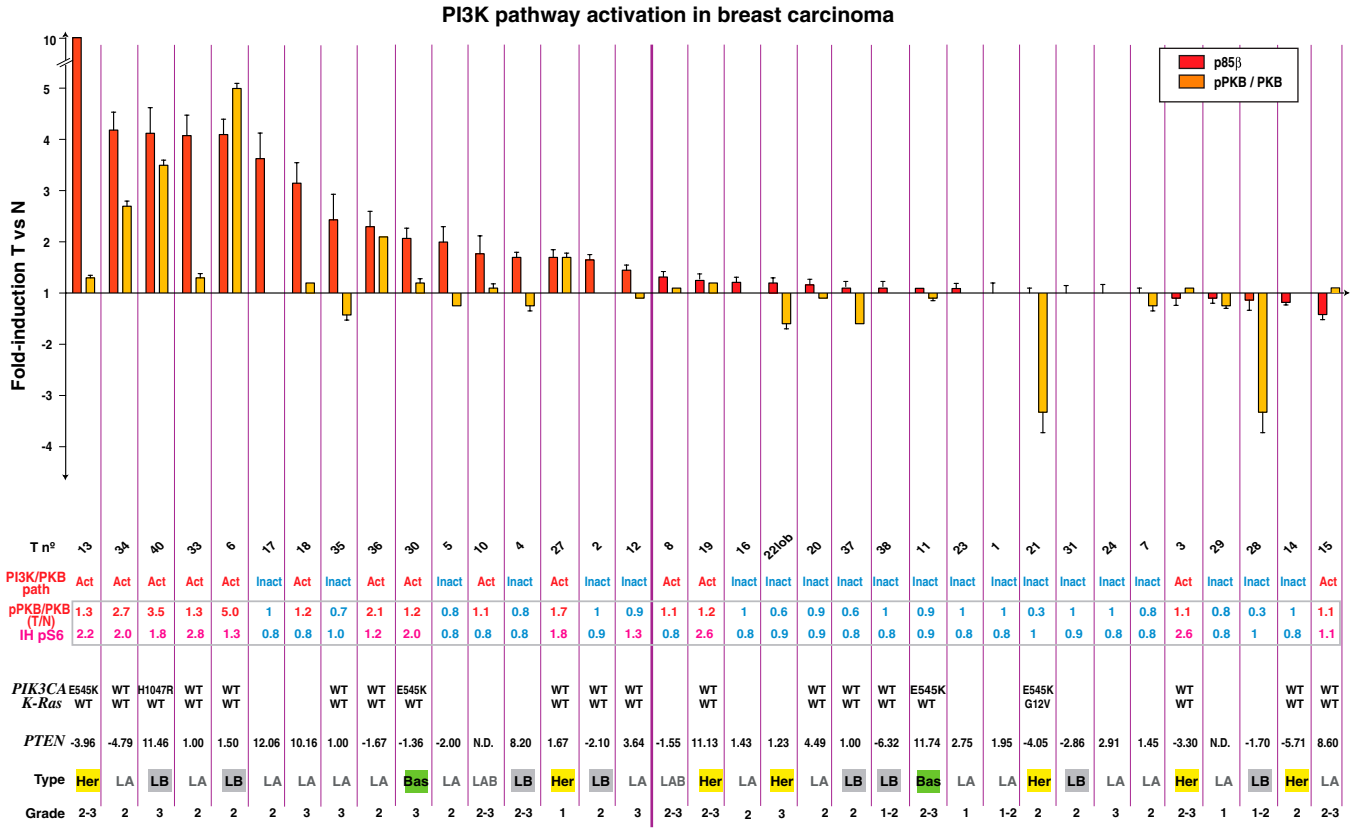

Fig. S3. p85β expression and PI3K pathway status in BC. p85β and pPKB/PKB levels in tumor (T) vs. surrounding normal (N) tissue was examined in WB by using appropriate Abs (triplicates). p85β WB signal intensity was normalized to that of actin, and the ratio of p85β signal intensity in tumor vs. normal tissue was obtained. pPKB was normalized to PKB, and PKB to actin; the ratio of pPKB/PKB value in tumor vs. normal tissue was obtained. The figure shows mean ± SD (n = 3–4 tests). Numbers <1 (decreased expression) are represented as their inverse negative values. Horizontal dashed line indicates a p85β change in the tumor of greater or less than 1.5-fold. Thick vertical line separates tumors with >1.5-fold increase in p85β compared with normal tissue. Beneath the graph, the following are indicated: tumor sample number, PI3K/PKB pathway status (active, Act; inactive, Inact), the specific *PIK3CA* and *K-Ras* point mutations, *PTEN* mRNA changes in T vs. N, tumor type [luminal A or B (LA, LB), luminal A or B (LAB), HER2 (Her2), or basal (Bas)], and Bloom–Richardson grade (grades 1–3). Sample 22 is an infiltrating lobular carcinoma; the remainder are infiltrating ductal carcinomas.

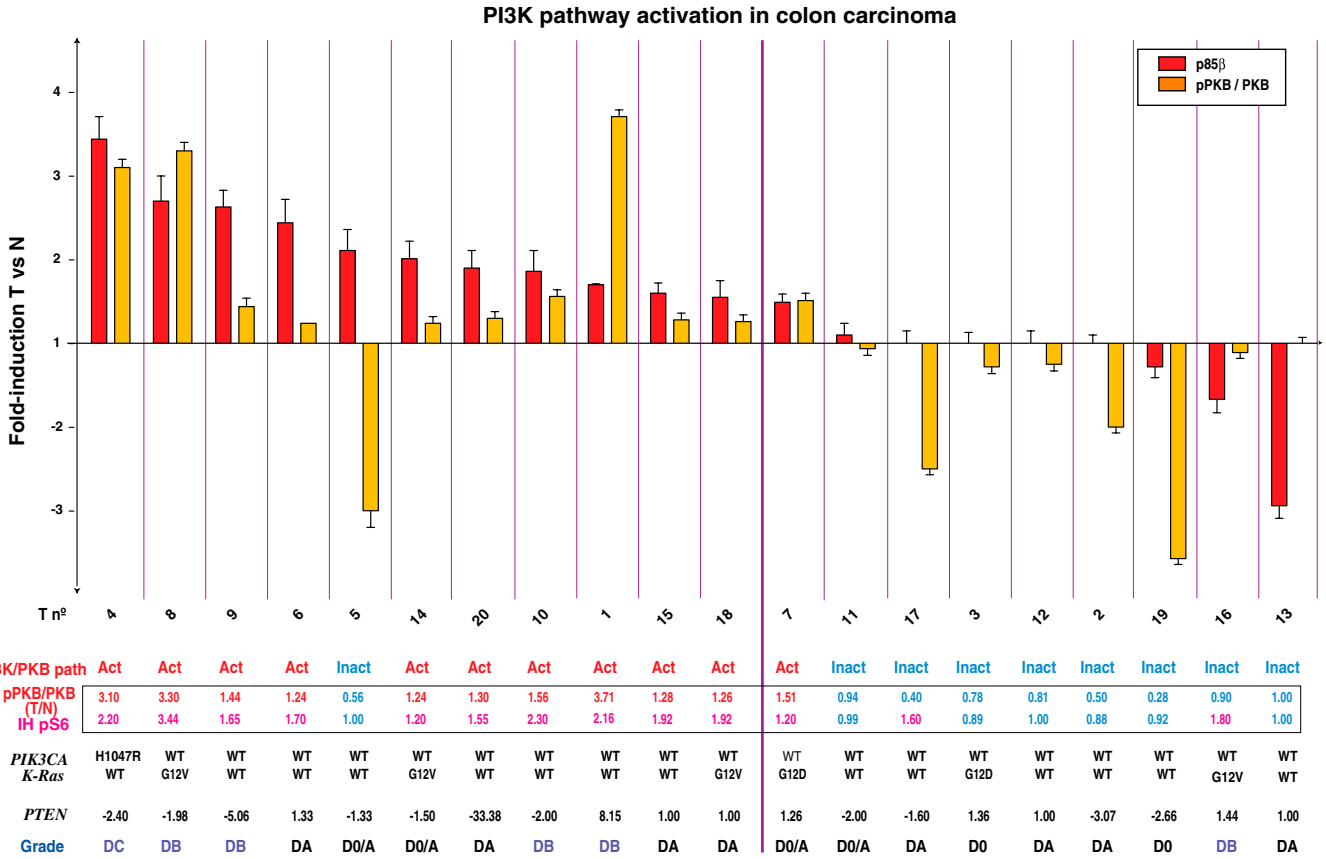

T nº	4	8	9	6	5	14	20	10	1	15	18	7	11	17	3	12	2	19	16	13
PI3K/PKB path	Act	Act	Act	Act	Inact	Act	Act	Act	Act	Act	Act	Act	Inact	Inact	Inact	Inact	Inact	Inact	Inact	Inact
pPKB/PKB (T/N)	3.10	3.30	1.44	1.24	0.56	1.24	1.30	1.56	3.71	1.28	1.26	1.51	0.94	0.40	0.78	0.81	0.50	0.28	0.90	1.00
IH pS6	2.20	3.44	1.65	1.70	1.00	1.20	1.55	2.30	2.16	1.92	1.92	1.20	0.99	1.60	0.89	1.00	0.88	0.92	1.80	1.00
PIK3CA	H1047R	WT	WT	WT	WT	WT	WT	WT	WT	WT	WT	WT	WT	WT	WT	WT	WT	WT	WT	WT
K-Ras	WT	G12V	WT	WT	WT	G12V	WT	WT	WT	WT	G12V	G12D	WT	WT	G12D	WT	WT	WT	G12V	WT
PTEN	-2.40	-1.98	-5.06	1.33	-1.33	-1.50	-33.38	-2.00	8.15	1.00	1.00	1.26	-2.00	-1.60	1.36	1.00	-3.07	-2.66	1.44	1.00
Grade	DC	DB	DB	DA	D0/A	D0/A	DA	DB	DB	DA	DA	D0/A	D0/A	DA	D0	DA	DA	D0	DB	DA

Fig. S4. p85β expression and PI3K pathway status in colon carcinoma. p85β and pPKB/PKB levels in CC were examined as in Fig. S3. Beneath the graph, the following are indicated: tumor number, PI3K pathway status (active, Act; inactive, Inact); *PIK3CA* and *K-Ras* point mutations, *PTEN* mRNA [tumor (T)-to-normal (N) ratios], and tumor grade (modified Dukes criteria, D0 to DC). Low *PTEN* mRNA levels in CC20 suggest a *PTEN* deletion as confirmed in WB; in CC 16 and 17, p70S6K activation was confirmed in WB.

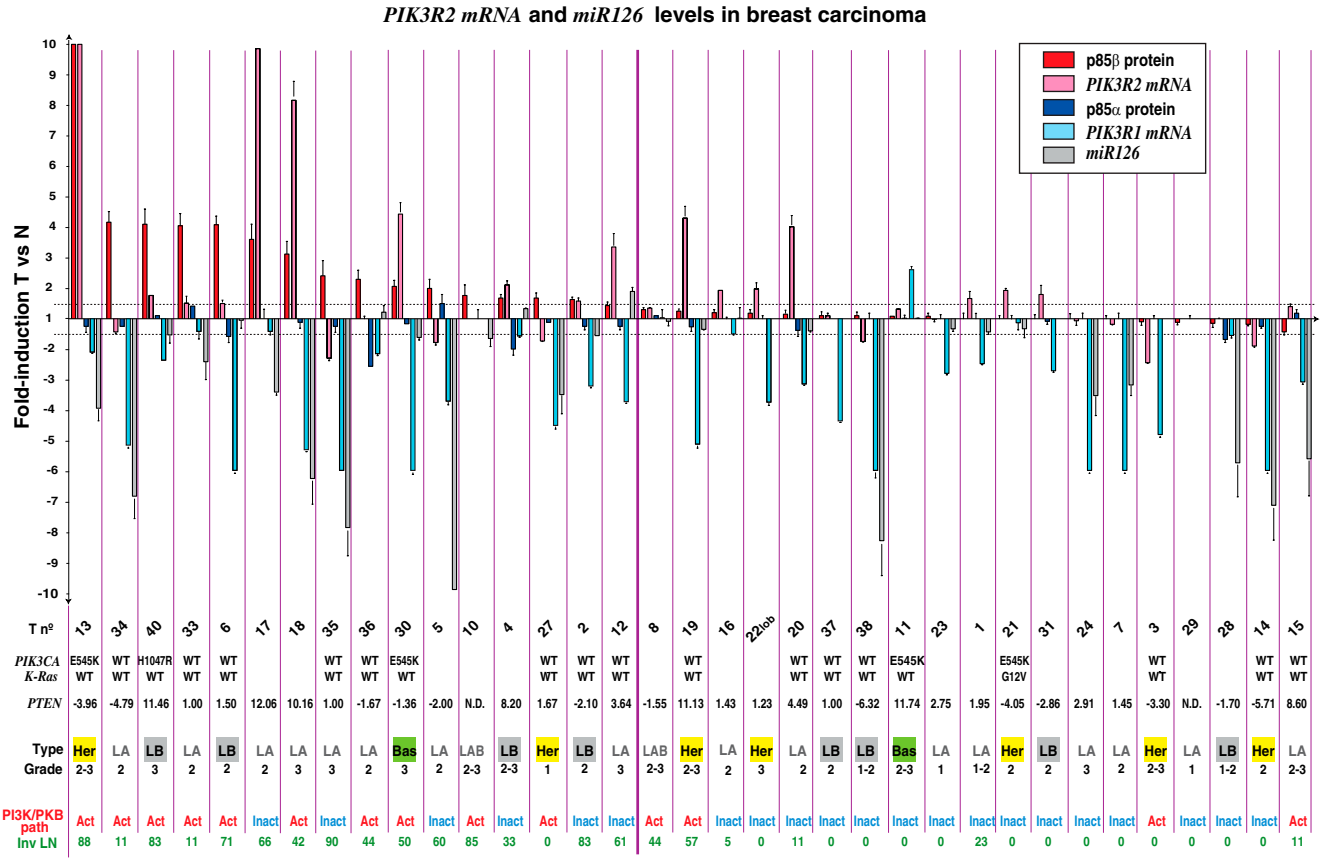

Fig. S5. p85α, p85β, *PIK3R1*, *PIK3R2*, and *miR126* levels in BC. The figure illustrates p85α and p85β protein levels, *PIK3R1* and *R2* mRNA content, and *miR126* levels in BC samples. p85 values were examined as in Fig. S3. *PIK3R1* and *R2* mRNA as well as *miR126* levels were examined by qPCR. mRNA levels were normalized to *ACTB* and *GADPH*, and each tumor sample was compared with surrounding normal tissue. RQ values ($2^{-\Delta\Delta Ct}$) were calculated to estimate mRNA levels. Graphs show *miR126* RQ of each BC [tumor (T)] sample, normalized for *U6* snRNA and *RNU19* (U19) and compared with surrounding normal tissue (N). The graph shows mean ± SD of the values obtained; samples were examined four times (with triplicate samples). Because of limited sample amounts, qPCR of tumors 31, 34, 35, 37, 38, and 40 was compared with that of a normal tissue sample pool. Several qPCR controls comparing a single patient's tumor with its own normal tissue sample and with the normal pool gave similar results. In all cases, equal content in tumor and normal samples of mRNA or protein yielded a value of 1. Below the graph we included the tumor information as in Fig. S3 and the percentage of metastatic lymph nodes (LN).

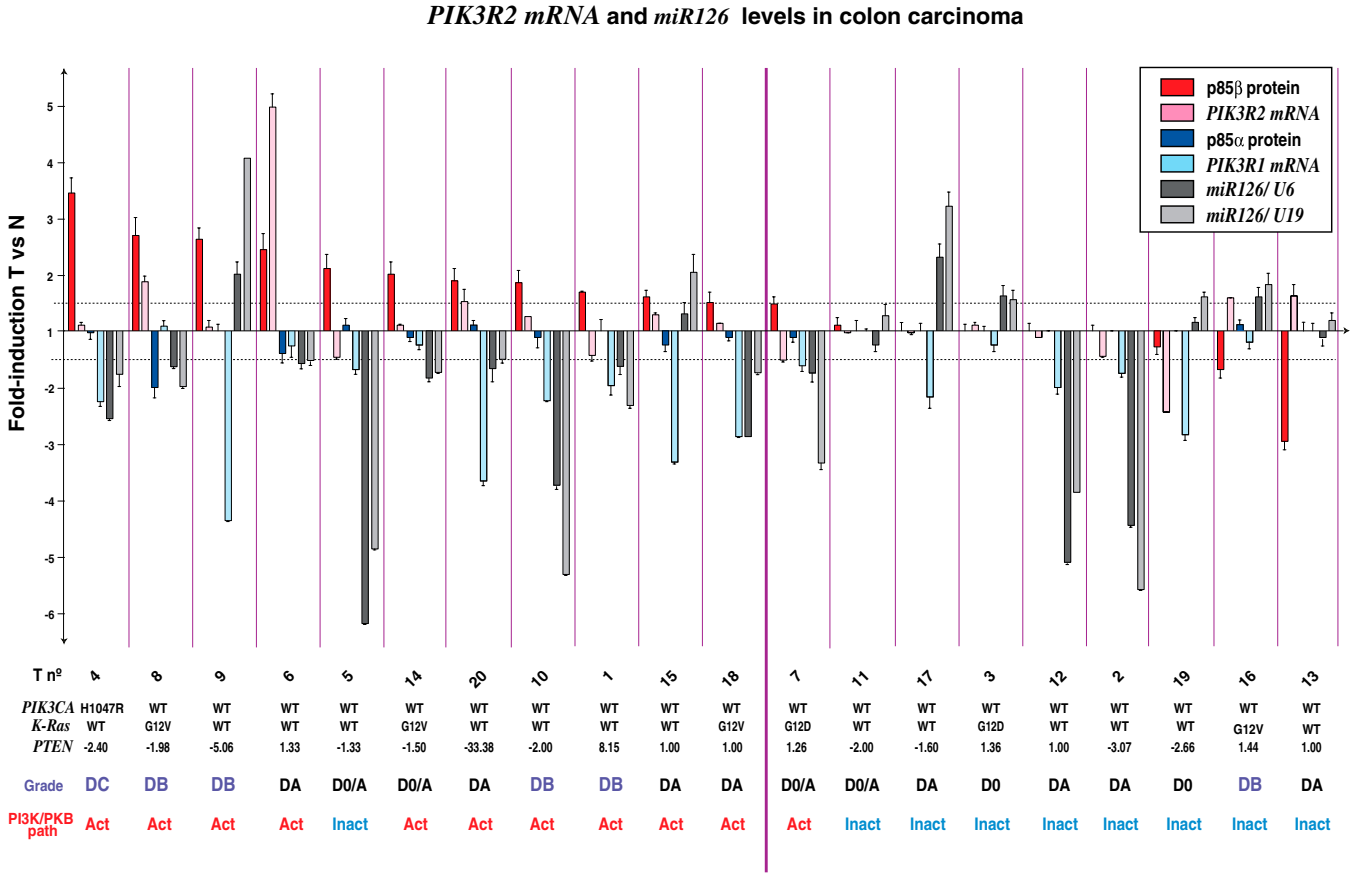

Fig. S6. p85 subunit expression, *PIK3R1* and *R2* mRNA, and *miR126* levels in colon carcinoma. p85α and p85β protein and *PIK3R1* and *R2* mRNA, as well as *miR126* levels, were examined as in Fig. S5. For *miR126* levels, values obtained with *U6* snRNA and *RNU19* (U19) controls are represented independently. Beneath the graph, tumor information is as in Fig. S4.

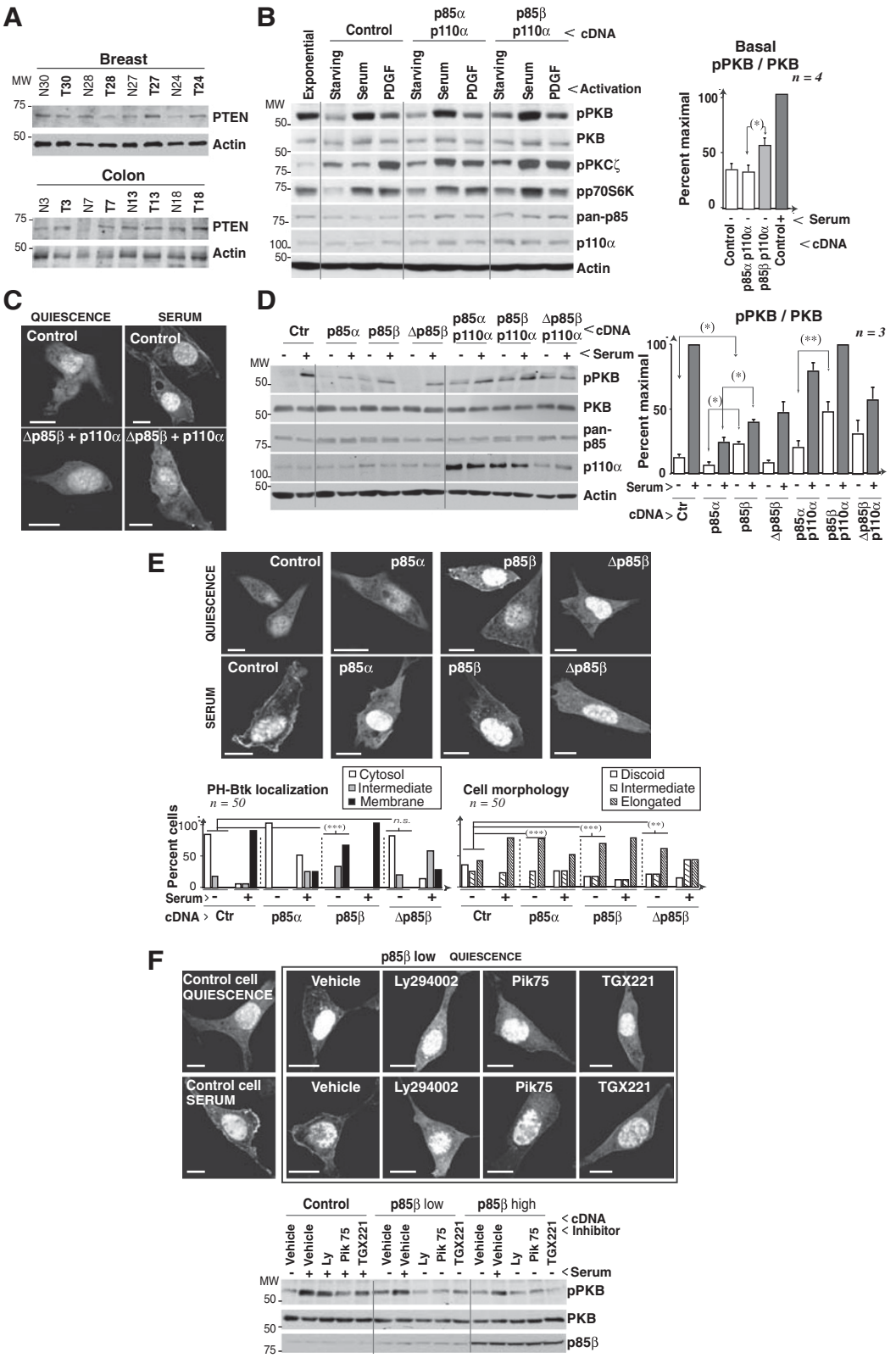

Fig. S7. p85β enhances PI3K pathway activation. (*A*) Extracts from representative CC and BC tumors (T) and surrounding normal tissue (N), were examined by WB using anti-PTEN Ab. PTEN protein levels examined in WB were consistent with *PTEN* mRNA levels examined by qPCR (in >90% of cases). (*B*) NIH 3T3 cells were transfected with empty control vector or cotransfected with pSG5-p110α and pSG5-p85α or -p85β. After 24 h, cells were incubated without serum (2 h) or stimulated with serum (10%) or PDGF (50 ng/mL; 10 min). Levels of PI3K subunits and PI3K effector activation were examined by WB. The graph shows quantification of the PI3K effector pPKB as the percentage of signal in each sample compared with maximum (100%, control with serum; mean ± SD, $n = 3$; *$P < 0.05$ by Student t test). (*C*) NIH 3T3 cells were transfected with EGFP-Btk-PH in combination with control vector or cDNAs encoding Δp85β/p110α (24 h), then incubated in serum-free medium (2 h) and activated with serum (15 min; as indicated). Btk-PH signal was examined by fluorescence microscopy. (*D*) NIH

Legend continued on following page

3T3 cells transfected with p85α, p85β, or Δp85β cDNAs alone or in combination with p110α (24 h) were incubated in serum-free medium for 2 h, and some were activated with serum for 15 min as indicated. Levels of PI3K subunits and PKB activation was examined as in *B*. (*E*) NIH 3T3 cells transfected with EGFP-Btk-PH in combination with p85α, p85β, or Δp85β (24 h) were examined as in *C*. Graphs and statistics are as in Fig. 3*B*. (*F*) Cells transfected p85β (24 h) were incubated in serum-free medium in the presence of a pan-PI3K inhibitor Ly29400 (5 μM), p110β inhibitor TGX221 (30 μM), or p110α inhibitor PIK75 (0.5 μM; 2 h). Cells were examined as in *E* or cell extracts as in *D*. (Scale bar: 15 μm.)

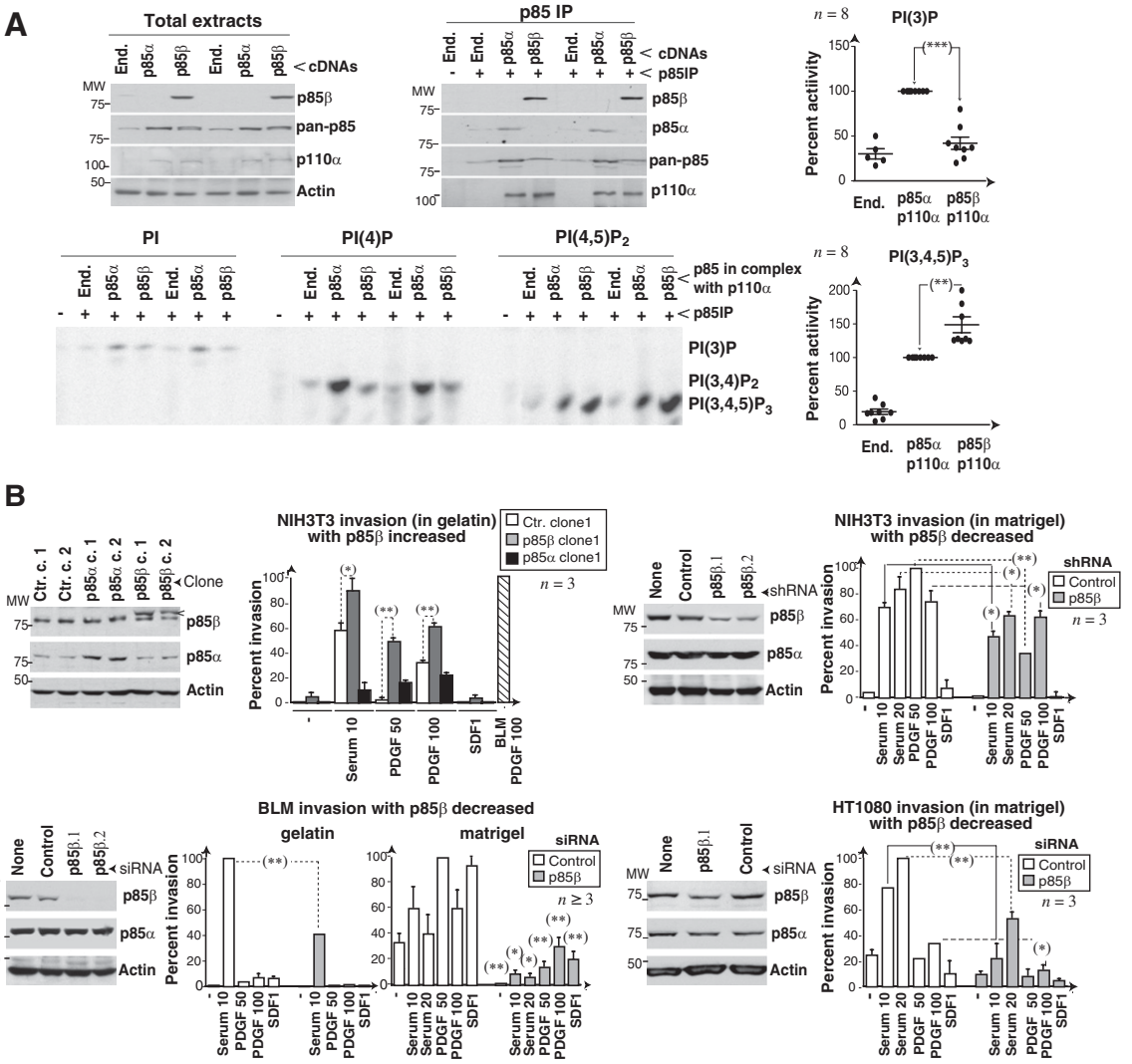

Fig. S8. p85β controls tumor invasion. (*A*) COS-7 cells were transfected with p85α/p110α or p85β/p110α (48 h). Total extracts were examined by WB or IP by using anti-p85 Ab (1C8 for p85β). IP-analyzed samples were tested in WB or in PI3K assays by using phosphatidylinositol (PtdIns) or PtdIns (4)P or PtdIns (4,5)P_2 as substrates (in duplicate). Graphs show percent activity in each sample compared with that of p85α/p110α (100%; $n = 8$; End, endogenous; $^{**}P < 0.01$ and $^{*}P < 0.05$ by Student *t* test). (*B*) Extracts of NIH 3T3 cell lines stably expressing control vector, p85α, or p85β, as well as extracts of NIH 3T3, BLM, or HT1080 cells transfected with control or p85β shRNA or siRNA (as indicated; 48 h) were examined by WB using appropriate Abs. In NIH 3T3 stable cell lines, p85β-specific band is indicated (arrowhead). Invasion assays were performed in gelatin or matrigel (as indicated) in the presence of serum (10% or 20%), PDGF (in ng/mL), or SDF-1 (100 ng/mL). The graphs show the percent cell invasion compared with maximal (100%; mean ± SD, $n = 3$; $^{*}P < 0.05$ and $^{**}P < 0.01$ by Student *t* test).

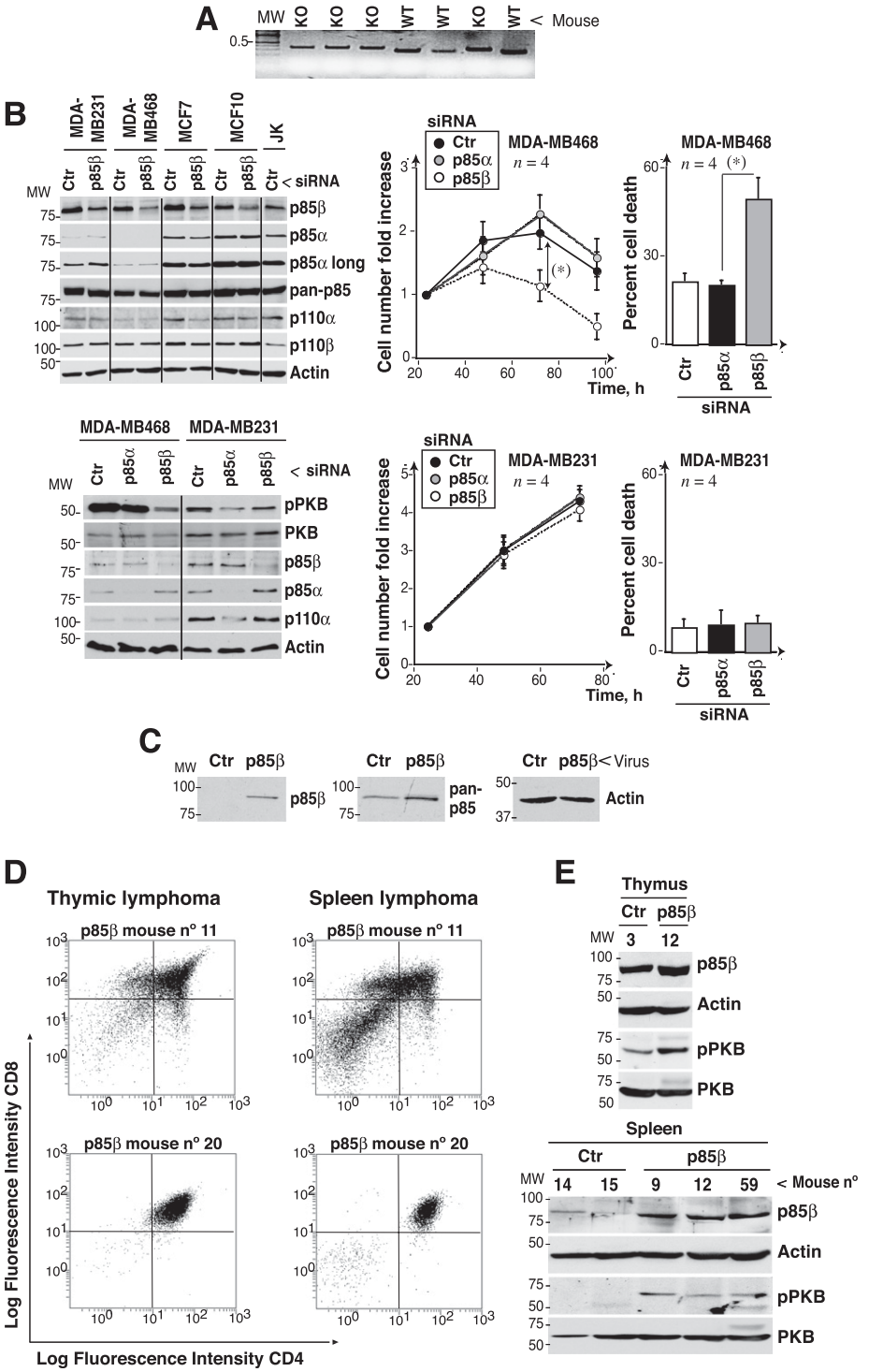

Fig. S9. Modulation of p85β expression in tumor samples. (*A*) Representative PCR of C57BL/6 p85β$^{+/+}$ and p85β$^{-/-}$ mice. (*B*) MCF10 normal immortal epithelial cells or BC cell lines MCF7, MDA-MB231, and MDA-MB 468 were transfected with control or p85β siRNA (48 h), and WB was used to check the p85α and p85β expression levels compared with Jurkat cells (p85α and p85β, ∼1:1) and the efficiency of p85β knockdown (*Upper*). MDA-MB231 and MDA-MB 468 cells were also transfected with p85α or p85β siRNA (48 h), and extracts were examined in WB (*Lower*). The graphs represent the MDA-MB231 and -MB468 cell count at indicated times after p85α or p85β siRNA transfection, as well as the percentage of cell death at 72 h. (*C*) SCID mouse BM cell suspensions were infected with control or p85β-encoding retrovirus (7 d); FACS analysis showed similar infection efficiency in all samples; p85β expression was tested in WB. (*D*) Flow cytometry analysis shows CD4 and CD8 surface marker expression in cells isolated from two representative thymic and spleen lymphomas of ENU-treated SCID mice (mouse number indicated) after adoptive transfer of BM cells overexpressing p85β. SCID mouse T cells are negative for CD3, CD4, and CD8; however, in mouse 11, the cells express CD4 and CD8 with a similar pattern in spleen and thymus. Mouse 20 represents another case with similar CD4 and CD8 expression pattern in spleen and thymus. In addition, in mouse 11, both organs expressed CD3, whereas, in mouse 20, neither spleen nor thymus expressed CD3. The similar phenotype of the cells in spleen and thymus suggests that the spleen cells derive from the thymic lymphoma. (*E*) WB shows p85β protein expression and pPKB levels in tumor extracts from representative control and p85β-transduced ENU-treated SCID mice.